

Mycobacterium tuberculosis evades macrophage defenses by inhibiting plasma membrane repair

Maziar Divangahi^{1,3}, Minjian Chen^{1,3}, Huixian Gan¹, Danielle Desjardins¹, Tyler T Hickman¹, David M Lee¹, Sarah Fortune², Samuel M Behar^{1,3} & Heinz G Remold^{1,3}

Induction of macrophage necrosis is a strategy used by virulent *Mycobacterium tuberculosis* (Mtb) to avoid innate host defense. In contrast, attenuated Mtb causes apoptosis, which limits bacterial replication and promotes T cell cross-priming by antigen-presenting cells. Here we show that Mtb infection causes plasma membrane microdisruptions. Resealing of these lesions, a process crucial for preventing necrosis and promoting apoptosis, required translocation of lysosomal and Golgi apparatus-derived vesicles to the plasma membrane. Plasma membrane repair depended on prostaglandin E₂ (PGE₂), which regulates synaptotagmin 7 (Syt-7), the calcium sensor involved in the lysosome-mediated repair mechanism. By inducing production of lipoxin A₄ (LXA₄), which blocks PGE₂ biosynthesis, virulent Mtb prevented membrane repair and induced necrosis. Thus, virulent Mtb impairs macrophage plasma membrane repair to evade host defenses.

Metazoan cells inhabit environments frequently subjected to mechanical stress, such as the stress that occurs in skin, gut and muscle¹, or as a consequence of interactions with pathogens^{2,3}, which can result in plasma membrane lesions. To ensure survival, cells rapidly repair membrane damage. Resealing of the plasma membrane is a ubiquitous and highly conserved process based on the exocytosis of endomembranes^{1,4}. Although Golgi-derived vesicles have been linked to membrane repair⁵, the most thoroughly studied secretory vesicles involved in plasma membrane repair resemble lysosomes⁶. The exocytosis of lysosomes is induced by calcium and depends on the function of the calcium sensor synaptotagmin 7 (Syt-7; A002565)⁷⁻⁹. Whereas Syt-7 is the calcium sensor of the lysosome^{7,10}, neuronal calcium sensor-1 (NCS-1; A000957) is the main calcium sensor of the Golgi membranes^{11,12} and is involved in vesicle trafficking from the *trans*-Golgi network¹³.

Infection with *Mycobacterium tuberculosis* (Mtb), the causative agent of tuberculosis and the main source of mortality from chronic pulmonary bacterial infection⁹, occurs in the lung through phagocytosis of the pathogens by pulmonary macrophages. After infection, virulent Mtb blocks phagosome maturation by interrupting acidification and lysosome fusion, which creates a protected niche in the cell for bacterial replication¹⁴. Ultimately, intracellular infection with virulent Mtb leads to macrophage death by necrosis, a process characterized by plasma membrane lysis and escape of the pathogens into the surrounding tissue for a new cycle of infection. In contrast, avirulent strains of Mtb induce apoptosis, a process that leads to sequestration and killing of intracellular bacilli and acts as a bridge from the innate immune response to the adaptive immune response¹⁵.

The underlying mechanisms by which virulent Mtb induces necrosis or inhibits apoptosis in macrophages remain largely unknown. The host lipid mediators prostaglandin E₂ (PGE₂) and lipoxin A₄ (LXA₄) exert opposing effects on the modality of Mtb-induced cell death in macrophages¹⁶. Macrophages infected with attenuated Mtb produce only small amounts of LXA₄ and instead elaborate prostanoids, including PGE₂, that protect against macrophage necrosis and promote apoptosis. In contrast, virulent Mtb infection induces production of LXA₄, which inhibits PGE₂ synthesis and apoptosis and leads to macrophage necrosis. These eicosanoids are also important *in vivo*, as mice deficient in 5-lipoxygenase (5-LO; *Alox5*^{-/-} mice) that are unable to synthesize LXA₄ are more resistant to chronic infection with virulent Mtb¹⁷. In contrast, prostaglandin E synthase-deficient (*Ptges*^{-/-}) mice, which are unable to produce PGE₂, are more susceptible to virulent Mtb¹⁶. The potential importance of the 5-LO pathway in humans is emphasized by the association people with 5-LO alleles that have lower 5-LO activity and a lower risk of tuberculosis¹⁸.

Mtb is endowed with the specialized protein secretion system ESX-1, which is a type VII secretion system¹⁹. ESX-1 secretion is thought to be critical in pore formation in host cell membranes^{3,20}. We therefore considered that virulent Mtb induces macrophage necrosis by disruption of the plasma membrane and inhibition of lesion repair. As embryonic fibroblasts from Syt-7-deficient mice are defective in lysosomal exocytosis and resealing of plasma membrane lesions²¹, we further considered that Syt-7 is a lysosomal component needed for calcium-dependent exocytosis and repair of plasma membrane lesions in macrophages infected with Mtb.

¹Division of Rheumatology, Immunology and Allergy, Department of Medicine, Brigham and Women's Hospital, Harvard Medical School, Boston, Massachusetts, USA.

²Department of Immunology and Infectious Diseases, Harvard School of Public Health, Boston, Massachusetts, USA. ³These authors contributed equally to this work. Correspondence should be addressed to H.G.R. (hremold@rics.bwh.harvard.edu) or S.M.B. (sbehar@rics.bwh.harvard.edu).

Received 6 March; accepted 21 May; published online 28 June 2009; doi:10.1038/ni.1758

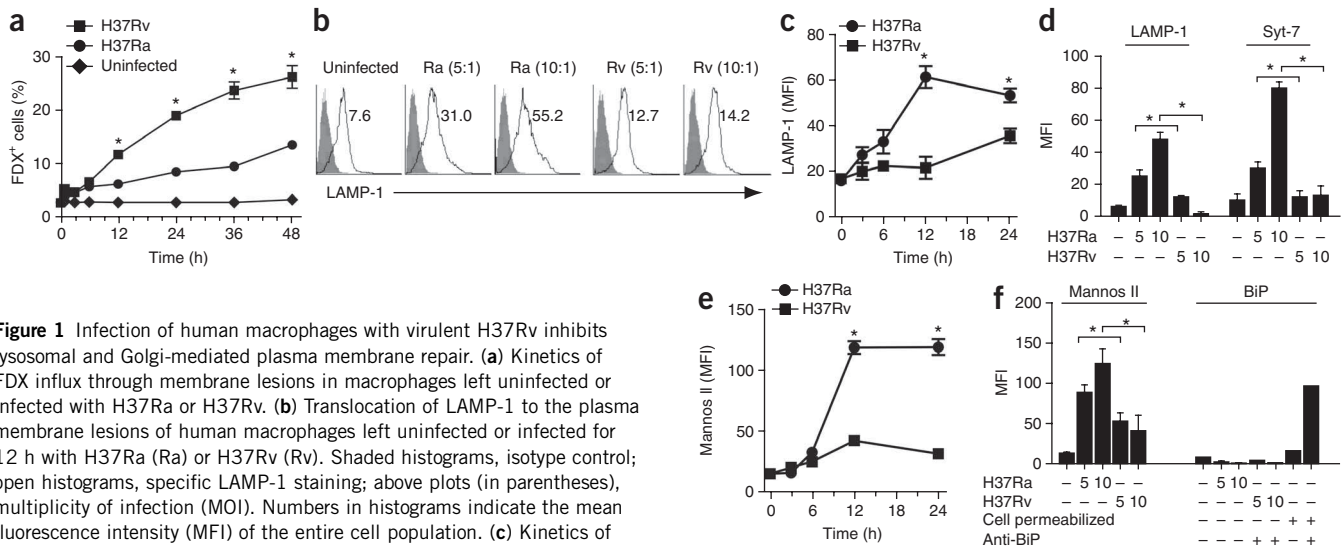


Figure 1 Infection of human macrophages with virulent H37Rv inhibits lysosomal and Golgi-mediated plasma membrane repair. **(a)** Kinetics of FDX influx through membrane lesions in macrophages left uninfected or infected with H37Ra or H37Rv. **(b)** Translocation of LAMP-1 to the plasma membrane lesions of human macrophages left uninfected or infected for 12 h with H37Ra (Ra) or H37Rv (Rv). Shaded histograms, isotype control; open histograms, specific LAMP-1 staining; above plots (in parentheses), multiplicity of infection (MOI). Numbers in histograms indicate the mean fluorescence intensity (MFI) of the entire cell population. **(c)** Kinetics of the translocation of LAMP-1 to the surface of human macrophages infected with H37Ra or H37Rv. **(d)** Translocation of LAMP-1 and Syt-7 to the surface of macrophages left uninfected or infected for 12 h with H37Ra or H37Rv. **(e)** Kinetics of the translocation of mannosidase II (Mannos II) as described in **c**. **(f)** Translocation of mannosidase II and the endoplasmic reticulum marker BiP as described in **d**; below, some macrophages were made permeable and/or stained with irrelevant antibody (Anti-BiP $-$) or BiP-specific antibody (Anti-BiP $+$). MOI, 10 (**a–c,e**) or as noted below graphs (**d,f**). * $P < 0.05$ (two-way analysis of variance (ANOVA; **a**) or t -test (**c–f**)). Data are representative of at least three independent experiments (error bars, s.e.m.).

Here we report that plasma membrane microdisruptions induced by attenuated Mtb were rapidly resealed by a repair mechanism that depended on recruitment of lysosomal and Golgi apparatus-derived membranes and resulted in apoptosis of infected macrophages. In contrast, virulent Mtb inhibited membrane repair and induced necrosis of the infected macrophage. Lysosome-dependent membrane repair was promoted by PGE₂ and, in the absence of PGE₂, infected macrophages were unable to control bacterial replication. Syt-7 is a critical gene product regulated by PGE₂, as in its absence, infected macrophages underwent necrosis and were unable to control Mtb growth.

RESULTS

Virulent Mtb causes persistent membrane microdisruptions

To determine whether Mtb induces plasma membrane disruptions, we evaluated the permeability of infected macrophages to FDX, a 75-kilodalton, inert, impermeant fluorescent molecule that enters the cytoplasm through membrane lesions^{22,23}. Beginning at 12 h after infection, there was significant influx of FDX into macrophages infected with virulent Mtb (strain H37Rv) and the FDX influx gradually increased with time. In contrast, there was significantly less influx of FDX into macrophages infected with avirulent Mtb (strain H37Ra; **Fig. 1a**). To exclude the possibility that enhanced accumulation of intracellular FDX was due to greater uptake of FDX by pinocytosis, we incubated macrophages with cytochalasin B, an inhibitor of pinocytosis; this treatment did not alter FDX influx after H37Rv infection (data not shown). These data collectively indicate that 12 h after infection with virulent H37Rv, persistent membrane lesions developed in infected macrophages.

The findings reported above could suggest that the membrane lesions inflicted by H37Ra were quickly resealed and that the lesions caused by H37Rv remained unrepaired. To determine whether lysosome recruitment is involved in membrane repair of H37Ra-infected macrophages and, if so, whether transport of lysosomal membranes

to the cell surface is inhibited in H37Rv-infected macrophages, we measured translocation of LAMP-1, a specific marker of late endosomes and lysosomes, to the cell surface²⁴. Macrophages infected with H37Ra showed significant translocation of LAMP-1 to the cell surface, which was visible as early as 3 h and was maximal by 12 h after infection (**Fig. 1b,c** and **Supplementary Fig. 1**). In contrast, we noted little or no translocation of LAMP-1 in macrophages infected with virulent H37Rv.

Lysosomal trafficking and exocytosis is dependent on Syt-7, the calcium-sensing protein located on late endosomes and lysosomes^{2,25}. Therefore, we investigated whether there was more cell surface Syt-7 after macrophage infection with avirulent H37Ra. Syt-7 expression on the macrophage surface was significantly greater after infection with H37Ra but not after infection with H37Rv (**Fig. 1d** and **Supplementary Fig. 1**). Because Golgi-derived membranes are also linked to plasma membrane resealing⁵, we next measured translocation of mannosidase II, a Golgi marker²⁶, to the cell surface. Mannosidase II expression increased on the macrophage plasma membrane starting at 12 h after H37Ra infection, but H37Rv-infected macrophages maintained low cell surface expression of mannosidase II (**Fig. 1e,f** and **Supplementary Fig. 1**). Conversely, endoplasmic reticulum-derived membranes were not involved in membrane repair, as the endoplasmic reticulum marker GRP78 (also known as BiP)^{27,28} was not recruited to the macrophage surface after infection with either H37Ra or H37Rv (**Fig. 1f**).

To determine whether the higher expression of lysosomal and Golgi markers on the surface of infected macrophages was due to greater protein synthesis, we measured total mannosidase II, LAMP-1 and annexin-1 protein in macrophages infected with H37Ra or H37Rv. Annexin-1 is a phospholipid-binding anti-inflammatory protein present in many cell types. The total amount of these proteins were not altered in macrophages infected with either H37Ra or H37Rv (**Supplementary Fig. 2**), which indicated that the differences in redistribution of the lysosomal and Golgi membrane compartments were not due to differences in total protein synthesis. These results

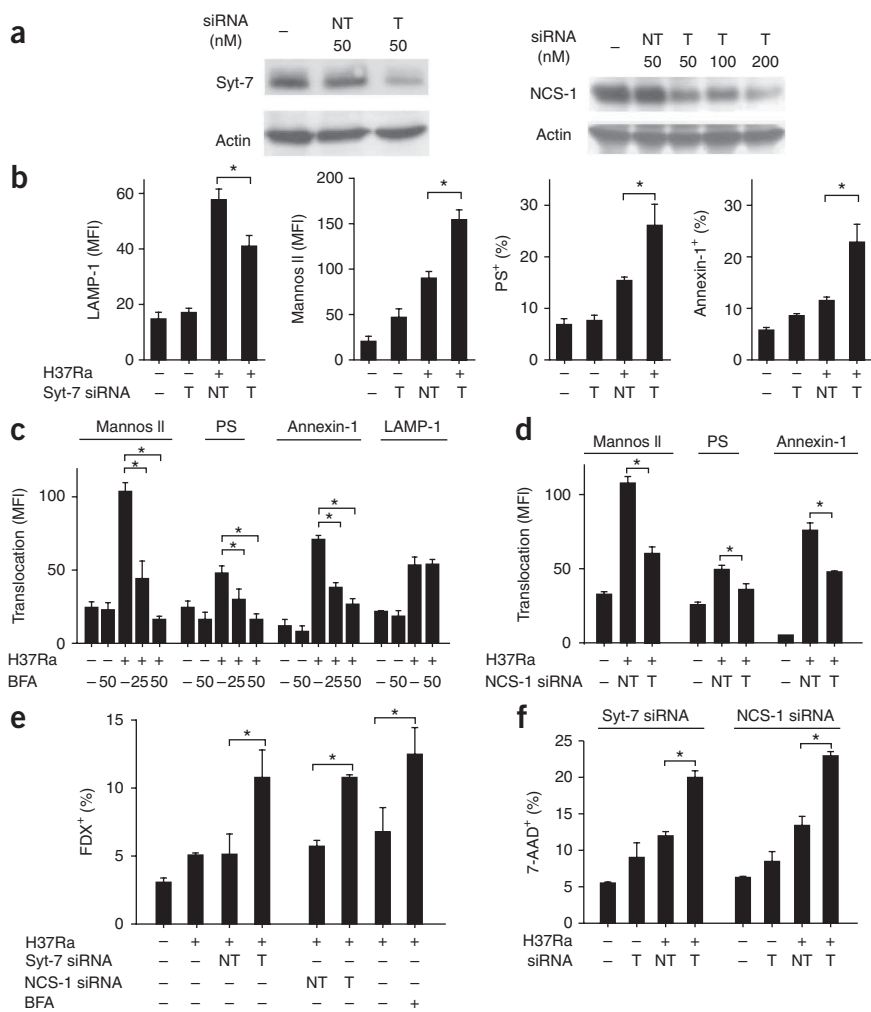


Figure 2 Distinct calcium sensors regulate the recruitment of lysosomal and Golgi apparatus-derived membranes in Mtb-infected human macrophages. (a) Immunoblot analysis of the expression of Syt-7 and NCS-1 before (–) and after gene silencing in human macrophages with targeting (T) or nontargeting (NT) siRNA. (b,c) Influence of Syt-7-specific siRNA (b) and brefeldin A (BFA; c) on the translocation of LAMP-1, mannose II, phosphatidylserine (PS) and annexin-1 to the surface of H37Ra-infected macrophages. (d) Influence of NCS-1-specific siRNA on the translocation of mannose II, phosphatidylserine and annexin-1 to the surface of H37Ra-infected macrophages. (e) Influx of FDX into H37Ra-infected macrophages expressing Syt-7- or NCS-1-specific siRNA or treated with BFA. (f) Necrosis of H37Ra-infected macrophages expressing Syt-7- or NCS-1-specific siRNA, assessed by staining with 7-amino-actinomycin D (7-AAD). MOI, 10. *, $P < 0.05$ (t -test). Data are from one representative of three independent experiments (error bars, s.e.m.).

macrophages infected with H37Ra in a dose-dependent way (Fig. 2c). In these conditions, translocation of LAMP-1-containing lysosomal membranes to the macrophage surface was not altered.

The experiments reported above suggested that Golgi apparatus-derived vesicles are recruited to the cell surface independently from lysosomal vesicles and that recruitment of the Golgi-derived membranes depends on a calcium sensor different from Syt-7. NCS-1 is a member of the EF family that has a calcium-binding motif^{12,32} and is especially abundant in Golgi apparatus-derived vesicles¹³.

NCS-1-specific siRNA (Fig. 2a) had an effect similar to brefeldin A, in that it resulted in inhibition of the translocation of Golgi membranes and significantly inhibited the translocation of phosphatidylserine and annexin-1 (Fig. 2d). These findings indicate that both lysosomal and Golgi-derived membranes move independently to the plasma membrane in infected macrophages.

To determine whether lysosome recruitment and Golgi membrane-derived vesicle recruitment are both important for the repair of plasma membrane damage, we tested whether lysosomal and Golgi membrane translocation were both required to prevent the influx of FDX into macrophages infected with H37Ra. Treatment with Syt-7-specific or NCS-1-specific siRNA or brefeldin A led to significantly greater influx of FDX into H37Ra-infected macrophages (Fig. 2e). In addition, Syt-7-specific and NCS-1-specific siRNA promoted macrophage necrosis after infection with H37Ra (Fig. 2f). Our data did not support the alternative explanation that instead of being quickly resealed, plasma membrane lesions are not generated by avirulent H37Ra (Fig. 2e,f). H37Ra caused considerable microdisruption of the plasma membrane when repair was inhibited. These data indicate that recruitment of lysosomal and Golgi membrane-derived vesicles is critical in the repair of plasma membrane damage after Mtb infection and is required to prevent necrosis.

PGE₂ promotes plasma membrane repair

The membrane-resealing process in fibroblasts is dependent on cAMP^{33,34}. We therefore investigated whether upregulation of cAMP concentrations is sufficient to trigger membrane repair. Treatment

collectively suggest that membranes from both the lysosomal and Golgi compartments are involved in macrophage plasma membrane resealing during avirulent mycobacterial infection.

Calcium sensors in plasma membrane repair

We next determined the function of calcium sensors in the recruitment of lysosomal and Golgi membranes to the cell surface of infected macrophages. Silencing of Syt-7 expression mediated by small interfering RNA (siRNA) impaired recruitment of lysosomal membranes to the macrophage surface after H37Ra infection (Fig. 2a,b). However, silencing of Syt-7 did not diminish and instead increased translocation of Golgi membranes to the macrophage surface (Fig. 2b), possibly due to a compensatory mechanism.

Phosphatidylserine and annexin-1 appear on the plasma membrane early during apoptosis to enable formation of the apoptotic envelope in macrophages infected with attenuated Mtb²⁹; this process is impaired in macrophages infected with virulent H37Rv³⁰. We therefore investigated whether translocation of Golgi membranes or lysosomal vesicles to the macrophage membrane surface was required for phosphatidylserine exocytosis and recruitment of annexin-1 to the macrophage surface. Syt-7-specific siRNA, which decreased translocation of LAMP-1 to the macrophage surface, enhanced rather than decreased expression of phosphatidylserine and annexin-1 on the macrophage surface (Fig. 2b). In contrast, brefeldin A, a highly specific inhibitor of Golgi membrane recruitment³¹, blocked the translocation of mannose II, phosphatidylserine and annexin-1 to the surface of

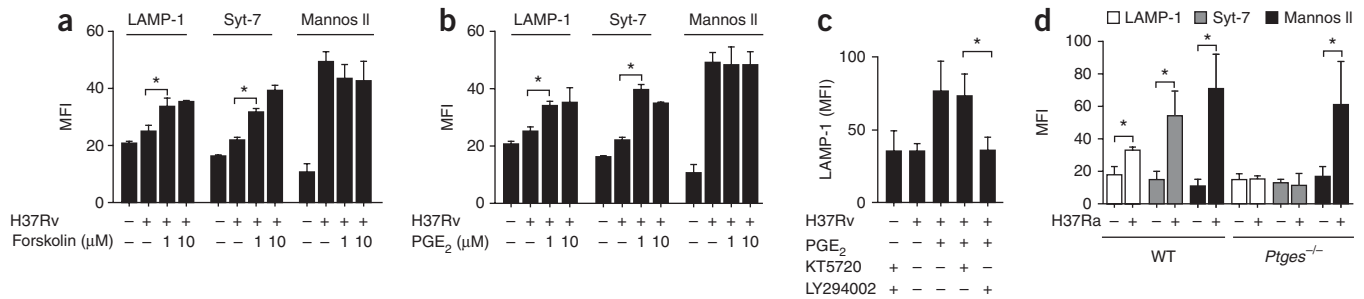


Figure 3 PGE₂ reconstitutes lysosomal repair in human macrophages infected with virulent *Mtb*. (**a,b**) Translocation of LAMP-1, Syt-7 and mannosidase II to the surface of macrophages infected with H37Rv (MOI, 10) and treated with 1–10 μM forskolin (**a**) or PGE₂ (**b**). (**c**) LAMP-1 translocation induced by H37Rv in the presence of PGE₂ after the addition of LY294002 (PI(3)K inhibitor) and/or KT5720 (PKA inhibitor). (**d**) Translocation of Syt-7, LAMP-1 and mannosidase II to the surface of H37Ra-infected wild-type (WT) and *Ptges*^{-/-} macrophages. **P* < 0.05 (*t*-test). Data are from one representative of three independent experiments (error bars, s.e.m.).

with forskolin, an activator of adenylate cyclase, resulted in greater translocation of LAMP-1- and Syt-7-containing membranes to the cell surface of H37Rv-infected macrophages but did not affect the translocation of Golgi membranes (Fig. 3a). PGE₂ exerts an important antinecrotic effect in infected macrophages by preventing perturbation of the mitochondrial inner membrane. This protective effect of PGE₂ on mitochondria is mediated by engagement of the PGE₂ receptor EP2, which induces the production of protein kinase A (PKA) and cAMP³⁰. In fact, the PGE₂ receptor EP2 and EP4, but not EP1 or EP3, both activate cAMP-dependent pathways³⁵. Therefore, we sought to determine whether induction of membrane repair, which is triggered by an increase in cAMP, is activated by PGE₂.

The exogenous addition of PGE₂ to H37Rv-infected macrophages reconstituted plasma membrane repair, as measured by enhanced translocation of LAMP-1 and Syt-7 to the cell surface (Fig. 3b,c). In contrast, PGE₂ did not affect the recruitment of mannosidase II-containing membranes. EP2 activates mainly PKA, whereas EP4 receptors activate phosphoinositide-3-OH kinase (PI(3)K)^{35,36}. To determine whether PGE₂-dependent activation of plasma membrane repair is caused by activation of PKA or PI(3)K, we assessed whether the specific PKA inhibitor KT5720 (ref. 37) and/or the PI(3)K inhibitor LY294002 (ref. 38) affect PGE₂-induced translocation of LAMP-1 to the plasma membrane of H37Rv-infected macrophages. LY294002 abrogated the translocation of LAMP-1 translocation to the cell surface of H37Rv-infected macrophages treated with PGE₂, whereas KT5720 had no effect (Fig. 3c). Either inhibitor alone had no effect on LAMP-1 translocation. Therefore, in contrast to the protective effects of PGE₂ on mitochondria, which depend on the EP2 receptor and ‘downstream’ activation

of PKA¹⁶, PGE₂-dependent lysosomal membrane translocation seems to require PI(3)K activation, which is typical of EP4 activation^{39,40}.

To further evaluate the function of PGE₂ in stimulating lysosome-dependent repair of plasma membranes, we infected mouse wild-type and *Ptges*^{-/-} splenic macrophages with H37Ra for 24 h. As expected, translocation of LAMP-1 and Syt-7 to the cell surface was significantly greater after infection with H37Ra in wild-type macrophages (Fig. 3d). In contrast, LAMP-1 and Syt-7 were not recruited to the plasma membrane of H37Ra-infected *Ptges*^{-/-} macrophages, which are unable to produce PGE₂ (Fig. 3d). We detected translocation of mannosidase II in both wild-type and *Ptges*^{-/-} macrophages. These data independently confirm that although recruitment of lysosomal membranes is PGE₂ dependent, recruitment of Golgi-derived membranes is independent of PGE₂. Notably, the propensity of *Ptges*^{-/-} macrophages to undergo necrosis when infected with H37Ra is reversed when exogenous PGE₂ is added¹⁶. These findings show the importance of PGE₂ in inducing lysosome-dependent repair of the plasma membrane.

Balance between LXA₄ and PGE₂ in control of *Mtb* infection

Infection of human macrophages with virulent *Mtb* induces LXA₄ synthesis, which leads to inhibition of PGE₂ production¹⁶. We

Figure 4 Bacterial growth and the death modality of *Mtb*-infected mouse macrophages is regulated by eicosanoids. (**a**) Enzyme-linked immunosorbent assay of apoptosis and necrosis 3 d after infection of *Alox5*^{-/-}, wild-type and *Ptges*^{-/-} macrophages with H37Rv (bottom) or H37Ra (top). (**b**) Replication of H37Rv (bottom) or H37Ra (top) at 4 h, 4 d or 7 d after infection (MOI 10:1) of *Alox5*^{-/-}, WT and *Ptges*^{-/-} macrophages. **P* < 0.05 (two-way ANOVA). Data are representative of three (**a**) and two (**b**) independent experiments (error bars, s.e.m.).

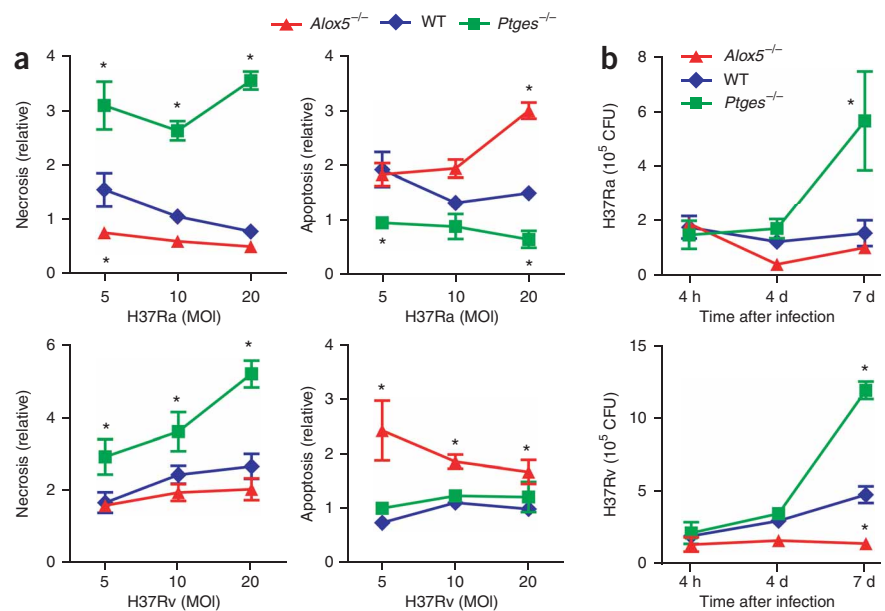
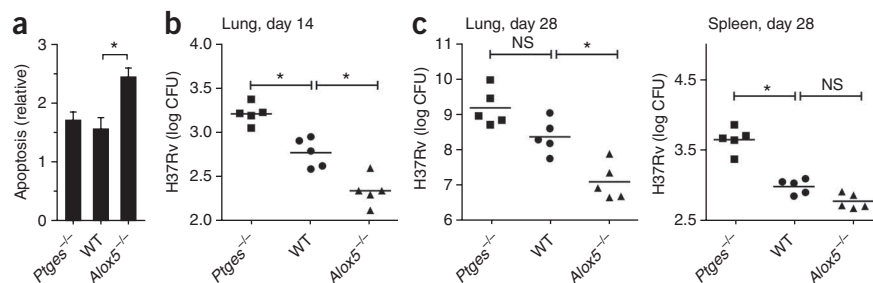


Figure 5 The fate of Mtb-infected macrophages *in vitro* reflects the innate control of infection *in vivo*. (a) Apoptosis of adherent antigen-presenting cells in bronchoalveolar lavage fluid collected 3 d after intratracheal infection of *Alox5*^{-/-}, *Ptges*^{-/-} and wild-type mice (*n* = 3 per group) with H37Rv (1×10^6 CFU). (b,c) Bacterial burden in the spleen and/or lung 14 d (b) and 28 d (c) after intratracheal transfer of H37Rv-infected *Alox5*^{-/-}, *Ptges*^{-/-} or wild-type macrophages into *Rag1*^{-/-} mice. Bacteria in lungs on day 1 after adoptive transfer: wild-type, log₁₀ = 1.81; *Ptges*^{-/-}, log₁₀ = 1.79; *Alox5*^{-/-}, log₁₀ = 1.8. **P* < 0.05 (one-way ANOVA). Data are from a single experiment with two time points (*n* = 5 mice per group per time point; error bars, s.e.m.).



sought to understand how PGE₂ and LXA₄ affect the outcome of Mtb infection. *Ptges*^{-/-} macrophages infected with avirulent H37Ra underwent significantly more necrosis and significantly less apoptosis than did wild-type or *Alox5*^{-/-} macrophages (which cannot produce LXA₄; **Fig. 4a**). We obtained the converse result with H37Ra-infected *Alox5*^{-/-} macrophages; these had more apoptosis and less necrosis than wild-type and *Ptges*^{-/-} macrophages. We obtained similar results with wild-type, *Alox5*^{-/-} and *Ptges*^{-/-} cells infected with virulent H37Rv.

Ptges^{-/-} and *Alox5*^{-/-} macrophages also showed substantial differences in the control of Mtb growth. H37Rv grew slowly in wild-type macrophages, increasing 2.5-fold after 7 d; in contrast, there was little replication of H37Rv in wild-type macrophages (**Fig. 4b**). The growth of virulent H37Rv was significantly lower in *Alox5*^{-/-} macrophages, whereas the growth of both H37Ra and H37Rv was enhanced in *Ptges*^{-/-} macrophages.

Alox5^{-/-} mice are more resistant¹⁷ and *Ptges*^{-/-} mice are more susceptible¹⁶ to virulent mycobacterial infection. However, the question of whether the mechanisms we have delineated *in vitro* are reflective of *in vivo* pathophysiology is difficult to answer, as the fate of infected macrophages can affect host resistance in many different ways^{41,42}. To determine whether more apoptosis occurs in the lungs of *Alox5*^{-/-} mice after virulent Mtb infection, we infected *Ptges*^{-/-}, wild-type and *Alox5*^{-/-} mice by the intratracheal route with 1×10^6 colony-forming units (CFU) of H37Rv and obtained cells by pulmonary lavage 3 d after infection. Cells from the lungs of *Alox5*^{-/-} mice underwent more apoptosis than did those from wild-type or *Ptges*^{-/-} mice (**Fig. 5a**).

To study the consequences of macrophage function on innate immunity to Mtb, we developed an experimental model involving the adoptive transfer of Mtb-infected macrophages. The advantage of this model is that it avoids the complications of analyzing knockout mice in which the deleted gene is expressed ubiquitously and affects several physiological processes. Thus, it allows specific determination of how manipulation of the lipid mediators produced by Mtb-infected macrophages alters the outcome of infection independently of their function in other cell types. We infected wild-type, *Alox5*^{-/-} and *Ptges*^{-/-} macrophages *in vitro* with a low dose of virulent H37Rv Mtb, then transferred the cells by the intratracheal route into recipient mice deficient in recombina-activating gene 1 (*Rag1*^{-/-} mice). By transferring the cells into *Rag1*^{-/-} recipient mice, we could evaluate the functional effect of eicosanoid regulation in the absence of any contribution from the adaptive immune system.

Two weeks after adoptive transfer, the pulmonary bacterial burden was significantly higher in *Rag1*^{-/-} mice that received infected *Ptges*^{-/-} macrophages than in recipients of infected wild-type macrophages (**Fig. 5b**). In contrast, the bacterial burden was significantly lower in *Rag1*^{-/-} mice that received infected *Alox5*^{-/-} macrophages than in

those that received infected wild-type macrophages (**Fig. 5b**). This effect was durable and was detected 28 d after transfer of the infected macrophages in the lungs as well as in the spleen (**Fig. 5c**). The mean difference in the pulmonary bacterial burden of *Rag1*^{-/-} mice that received *Alox5*^{-/-} macrophages and those that received wild-type macrophages was $\Delta \log_{10} = 1.3$ (*P* < 0.05). These experiments show that transfer of infected *Alox5*^{-/-} macrophages (which are predisposed to apoptosis after infection) into *Rag1*^{-/-} mice restricts virulent Mtb replication *in vivo*. The use of *Rag1*^{-/-} recipient mice shows that this effect is determined by the macrophage genotype and is independent of adaptive immunity. Thus, the balance of PGE₂ and LXA₄ production by infected macrophages affects the outcome of infection in the microenvironment of the lung.

Induction of Syt-7 transcription by PGE₂

We have shown that Syt-7 is a central regulator of calcium-dependent translocation of lysosomal membranes to the cell surface and is required for successful membrane repair and prevention of necrosis in human macrophages. We have also shown that PGE₂ is indispensable for the induction of lysosome translocation to the macrophage surface and plasma membrane repair in Mtb-infected macrophages. We next investigated whether PGE₂ is involved in Syt-7 synthesis. For this, we quantified Syt-7 mRNA transcripts in uninfected macrophages in the presence and absence of PGE₂. Although we did not detect Syt-7 transcripts in uninfected macrophages, the addition of PGE₂ induced Syt-7 expression in a dose- and time-dependent way (**Fig. 6a**). In contrast, LAMP-1 transcription was not substantially affected when exogenous PGE₂ was added to uninfected macrophages (**Fig. 6b**). We next sought to determine whether exogenous PGE₂ increases Syt-7 transcript abundance in H37Rv-infected macrophages. H37Rv infection and exogenous PGE₂ synergistically increased Syt-7 transcript abundance (**Fig. 6c**). The abundance of LAMP-1 transcript was not affected in these conditions. These findings provide a mechanistic link between the ability of PGE₂ to induce Syt-7, a critical regulator of lysosome translocation, to plasma membrane lesions and its ability to stimulate membrane repair.

As expected, *Alox5*^{-/-} macrophages infected with H37Rv expressed more Syt-7 than did wild-type or *Ptges*^{-/-} macrophages infected with H37Rv (**Fig. 6d**). Syt-7 expression was induced only transiently in wild-type and *Ptges*^{-/-} macrophages infected with virulent Mtb. LAMP-1 expression was not affected by infection with virulent Mtb or by the ability of the macrophages to produce eicosanoids (**Fig. 6d** and **Supplementary Fig. 2**).

We confirmed the findings reported above with *in vivo* experiments. At 7 d after aerosol infection with a low dose of H37Ra, wild-type mice had a greater abundance of Syt-7 transcripts in their lungs, whereas mice infected with virulent Mtb had smaller quantities of Syt-7 mRNA that were similar to those in uninfected mice (**Fig. 6e**).

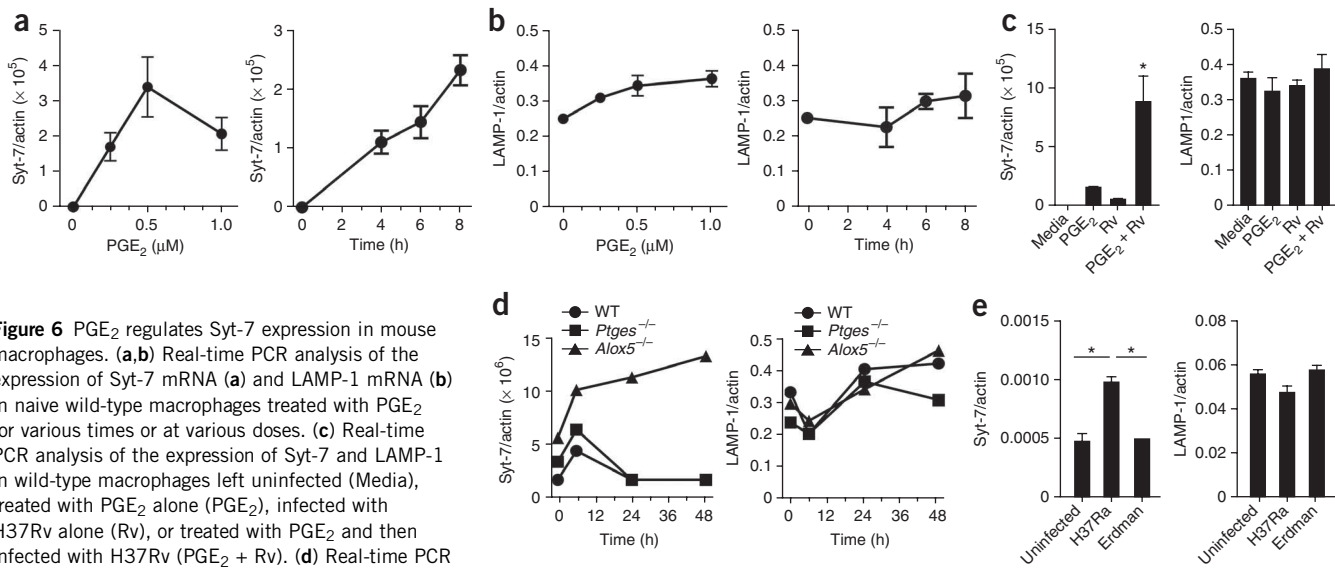


Figure 6 PGE₂ regulates Syt-7 expression in mouse macrophages. **(a,b)** Real-time PCR analysis of the expression of Syt-7 mRNA **(a)** and LAMP-1 mRNA **(b)** in naive wild-type macrophages treated with PGE₂ for various times or at various doses. **(c)** Real-time PCR analysis of the expression of Syt-7 and LAMP-1 in wild-type macrophages left uninfected (Media), treated with PGE₂ alone (PGE₂), infected with H37Rv alone (Rv), or treated with PGE₂ and then infected with H37Rv (PGE₂ + Rv). **(d)** Real-time PCR analysis of the expression of Syt-7 and LAMP-1 mRNA in *Alox5*^{-/-}, *Ptges*^{-/-} and wild-type macrophages 0–48 h (horizontal axis) after infection with H37Rv. **(e)** Real-time PCR analysis of the expression of Syt-7 and LAMP-1 mRNA in lungs of wild-type mice left uninfected or infected by the aerosol route with a low dose (~100 CFU) of H37Ra or the Erdman strain of Mtb; RNA was extracted from whole lung 7 d after infection. Expression of Syt-7 or LAMP-1 is presented relative to β-actin expression. **P* < 0.05 (one-way ANOVA). Data are from one experiment representative of two **(a–c,f)** or three **(d,e)** independent experiments (*n* = 3 mice per group; error bars, s.e.m.).

LAMP1 expression was not affected by infection. These data collectively show that virulent Mtb evades innate immunity by suppressing the production of PGE₂ (ref. 16), which is required for optimal expression of Syt-7 and lysosome-dependent plasma membrane repair.

Syt-7 is essential for control of virulent Mtb

We have established the importance of eicosanoids in determining the cellular fate of Mtb-infected macrophages, which determines whether the bacteria succumb to or evade innate immune control (Figs. 4 and

5). The finding that Syt-7 is regulated by PGE₂ (Fig. 6) indicates a mechanism by which PGE₂ induces membrane repair (Fig. 3). We next sought to show a direct link among Syt-7 function, the death modality of Mtb-infected macrophages and the outcome of infection. Because our data indicated that one consequence of LXA₄ induction by virulent Mtb is inhibition of Syt-7 transcription, we predicted that *Alox5*^{-/-} macrophages, which accumulate Syt-7 transcripts after infection (Fig. 6d), would have enhanced membrane repair after H37Rv infection.

We detected translocation of LAMP-1 to the cell surface after H37Rv infection in *Alox5*^{-/-} macrophages but not in wild-type or *Ptges*^{-/-} macrophages (Fig. 7a). To directly visualize whether there was enhanced plasma membrane repair in *Alox5*^{-/-} macrophages, we infected wild-type, *Ptges*^{-/-} and *Alox5*^{-/-} macrophages with green fluorescent protein (GFP)-labeled H37Rv, then labeled the surface of infected cells with an antibody specific for the luminal (extracellular) domain of LAMP-1. We detected little LAMP-1 on the surface of GFP-H37Rv-infected wild-type or *Ptges*^{-/-} macrophages (Fig. 7b). In contrast, GFP-H37Rv induced extensive recruitment of LAMP-1 to the surface of *Alox5*^{-/-} macrophages (Fig. 7b). The greater LAMP-1 staining reflected a true change in LAMP-1 recruitment to the cell

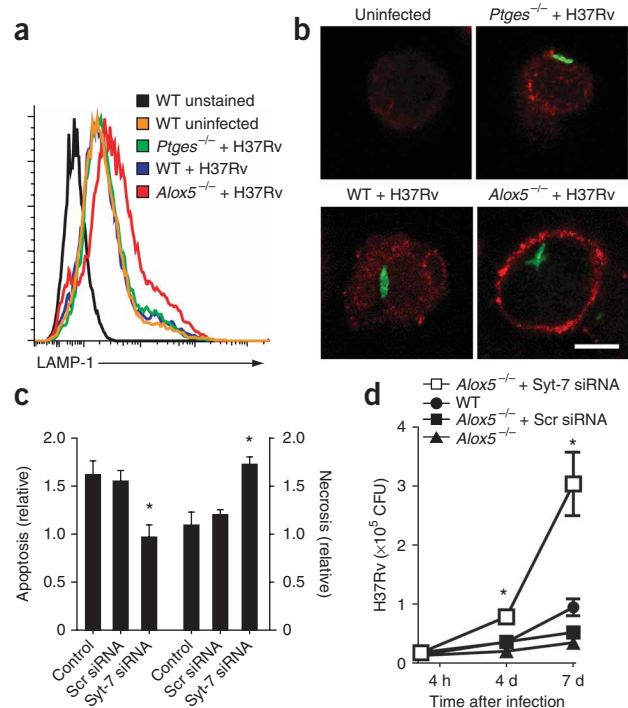


Figure 7 Syt-7 is essential for the induction of plasma membrane repair, prevention of necrosis and control of bacterial growth in mouse macrophages. **(a,b)** Flow cytometry **(a)** and confocal microscopy **(b)** showing translocation of LAMP-1 to the cell surface of *Alox5*^{-/-}, *Ptges*^{-/-} and wild-type macrophages left uninfected or 24 h after infection with H37Rv (MOI, 5). **(b)** Macrophages infected with GFP-labeled H37Rv (MOI, 10) and stained with monoclonal antibody to the luminal domain of LAMP-1 (no permeabilization). Scale bar, 5 μm. **(c)** Apoptosis and necrosis of *Alox5*^{-/-} macrophages left untransfected (control) or transfected for 24 h with scrambled (Scr) or Syt-7-specific siRNA, followed by H37Rv infection (MOI, 5) and analysis 3 d after infection; results are presented relative to those of uninfected cells. **(d)** H37Rv growth in wild-type and *Alox5*^{-/-} macrophages left untreated or transfected with Syt-7-specific or scrambled siRNA at 4 h, 4 d or 7 d after infection with H37Rv. *, *P* < 0.05 (one-way **(c)** or two-way **(d)** ANOVA). Data are representative of two independent experiments (error bars, s.e.m.).

surface, as wild-type, *Ptges*^{-/-} and *Alox5*^{-/-} macrophages all expressed similar amounts of intracellular LAMP-1 (Supplementary Fig. 3). These data indicate that of the larger amounts of PGE₂ in H37Rv-infected *Alox5*^{-/-} macrophages enhance lysosomal plasma membrane repair.

To show that Syt-7 expression has a direct influence on the death modality of the infected macrophages, we undertook gene silencing of Syt-7 in H37Rv-infected *Alox5*^{-/-} macrophages (Fig. 7c). Although H37Rv induced more apoptosis than necrosis in *Alox5*^{-/-} macrophages, Syt-7 silencing reversed this phenotype and resulted in significantly less apoptosis and more necrosis (Figs. 4a and 7c). Thus, Syt-7 seems to be critical in preventing necrosis and inducing apoptosis in macrophages infected with Mtb.

Finally, as *Alox5*^{-/-} macrophages have an enhanced ability to limit Mtb replication both *in vitro* and *in vivo* (Figs. 4 and 5), we sought to determine whether Syt-7 function is directly involved in innate control of Mtb infection. Although *Alox5*^{-/-} macrophages limited bacterial replication more efficiently than did wild-type macrophages, Syt-7 silencing significantly impaired the ability of *Alox5*^{-/-} macrophages to restrict bacterial replication and led to a significant increase in Mtb (Fig. 7d). Collectively, these data indicate that PGE₂ is an essential mediator that stimulates Syt-7 production to activate lysosome-dependent membrane repair, which prevents necrosis, instead leading to apoptosis and innate protection against Mtb infection.

DISCUSSION

Necrosis is a highly regulated irreversible loss of plasma membrane integrity. Although virulent Mtb has been shown to block the formation of the apoptotic envelope in infected macrophages and thereby lead to necrosis²⁹, the mechanisms that facilitate necrosis in this system have remained unknown. Here we found that virulent Mtb perturbs the repair of plasma membrane microdisruptions inflicted by the pathogen. We identified two distinct and essential components involved in plasma membrane repair: lysosomal and Golgi-derived vesicles. Although macrophages infected with attenuated Mtb underwent plasma membrane repair and apoptosis, blockade of the translocation of either lysosomal or Golgi apparatus-derived vesicles to the plasma membrane resulted in significant necrosis. Silencing of the calcium sensor Syt-7 inhibited lysosome-dependent repair of plasma membranes but did not affect the translocation of mannosidase II-containing Golgi-derived membranes. In contrast, silencing of NCS-1, a calcium sensor present in Golgi apparatus, significantly inhibited the translocation of Golgi-derived membranes and downregulated the translocation of phosphatidylserine and annexin-1 to the macrophage surface. Thus, two distinct calcium sensor proteins regulate lysosomal and Golgi-dependent plasma membrane repair in Mtb-infected macrophages. Although both lysosomal and Golgi apparatus-derived vesicles were required for membrane repair, only the Golgi vesicle-dependent membrane repair facilitated exocytosis of the apoptotic marker phosphatidylserine and deposition of annexin-1 on the cell surface. Golgi-derived vesicle-mediated membrane repair was PGE₂ independent, which indicates that other mediators are involved in the recruitment of these membranes to the plasma membrane lesions. Further study of the Golgi-derived vesicle membrane-repair pathway will considerably extend understanding of the biology of apoptosis.

Virulent H37Rv stimulates LXA₄ production in macrophages, which inhibits PGE₂ production by downregulation of the accumulation of mRNA encoding cyclooxygenase 2 (ref. 16). PGE₂ protects mitochondrial membranes from damage caused by Mtb infection and thereby inhibits necrosis. Here we have reported that PGE₂ production

restored translocation of lysosomal membranes to the cell surface in macrophages infected with virulent Mtb, and that PGE₂ upregulated synthesis of Syt-7 (ref. 7). Thus, PGE₂ activates at least two independent pathways that protect Mtb-infected macrophages from necrosis. First, PGE₂ acts on the PGE₂ receptor EP2, which stimulates adenylate cyclase to produce cAMP by activation of protein kinase A³⁶ and protects against Mtb-induced mitochondrial damage³⁰. Second, PGE₂ activates plasma membrane repair through PI(3)K, which most probably involves the EP4 receptor^{35,40}. Thus, PGE₂ protects Mtb-infected cells against necrosis by preventing mitochondrial inner membrane instability and plasma membrane disruption.

Even attenuated H37Ra was more virulent than when infecting *Ptges*^{-/-} macrophages than when infecting wild-type macrophages. Conversely, virulent H37Rv showed an attenuated phenotype when infecting *Alox5*^{-/-} macrophages, as PGE₂ production was not counter-regulated by LXA₄. Thus, in an intracellular milieu dominated by PGE₂, infected macrophages underwent more apoptosis and restricted Mtb growth. These findings indicate that the ability of host macrophages to produce PGE₂ modulates the virulence of Mtb. Therefore, the innate host response is able to modify the phenotypic expression of bacterial virulence.

Alox5^{-/-} mice were more resistant and *Ptges*^{-/-} mice were more susceptible than wild-type mice when infected by the aerosol route with Mtb^{16,17}. However, our transfer experiments showed that the fate of the infected macrophages was a key determinant of the relative resistance of these mice. Although *Alox5*^{-/-}, *Ptges*^{-/-} and wild-type macrophages were all infected to a similar degree, transfer of infected *Alox5*^{-/-} macrophages resulted in a much less severe systemic infection than did transfer of infected wild-type or *Ptges*^{-/-} macrophages. Therefore, the fate of transferred macrophages, whether apoptotic or necrotic, had a durable effect on the course of infection. This is the first direct demonstration to our knowledge that the death modality of infected macrophages alters the course of Mtb infection *in vivo*. Thus, we have provided a direct mechanistic link between the beneficial function of PGE₂ and outcome of infection.

Although we have gained some knowledge about the donor vesicles involved in plasma membrane repair of Mtb-infected macrophages and about the importance of calcium sensors in the regulation of plasma membrane repair, exactly how PGE₂ facilitates membrane repair remains unclear. Attenuated Mtb triggered PGE₂-dependent LAMP-1 translocation to the macrophage surface in a PI(3)K-dependent way. Phagosome-lysosome fusion is thought to be inhibited in Mtb-infected macrophages⁴³ by constant removal of phosphatidylinositol-3-phosphate from the endosomal membranes by SapM, a pathogen-derived phosphatase, in a way that is independent of cytosolic calcium⁴⁴. It is therefore likely that PGE₂ upregulates PI(3)K activity to generate sufficient phosphatidylinositol-3-phosphate for membrane repair. If pathogen-mediated depletion of phosphatidylinositol-3-phosphate affects both phagosome-lysosome fusion and plasma membrane repair, it could be assumed that plasma membrane repair and phagosome-lysosome fusion are mediated by related mediators. This observation is consistent with published work demonstrating that ESX-1 proteins are required for translocation of Mtb from the phagolysosome to the cytosol⁴⁵, and our finding that translocation of LAMP-1 to macrophage plasma membrane lesions also depended on *ESX1*-encoded proteins (data not shown). In addition, other studies have reported that the early intracellular survival of *Salmonella* and *Yersinia* is inhibited in mouse embryonic fibroblasts as a consequence of Syt-7-dependent phagosome-lysosome fusion².

Here we established a causal relationship between the capacity of macrophages to restrict mycobacterial growth and their ability to

reseal membrane lesions inflicted by the pathogen and to induce apoptosis. If membrane repair is prevented, infected macrophages are doomed to become necrotic and support enhanced bacterial growth. Thus, inhibiting membrane repair by blocking PGE₂ production represents a critical mechanism that allows virulent bacilli to replicate, induce necrosis and escape from the host macrophage and infect other cells. Better understanding of the mechanisms by which Mtb induces necrosis might identify new targets for drugs that modulate innate immune responses to control the initial infection as well as to enhance adaptive immunity.

METHODS

Methods and any associated references are available in the online version of the paper at <http://www.nature.com/natureimmunology/>.

Accession codes. UCSD-Nature Signaling Gateway (<http://www.signaling-gateway.org>): A002565 and A000957.

Note: Supplementary information is available on the Nature Immunology website.

ACKNOWLEDGMENTS

We thank I.-C. Ho for critical reading of the manuscript; and B. Koller (University of North Carolina) for *Piges*^{-/-} mice. Supported by the US National Institutes of Health (AI50216 and AI072143 to H.G.R.) and the Fonds de la Recherche en Santé du Québec (M.D.).

AUTHOR CONTRIBUTIONS

S.M.B., H.G.R. and M.D. conceived of and designed the experiments, analyzed the data and wrote the paper; M.D., M.C. and H.G. did the experiments with assistance from D.D.; T.T.H. did confocal microscopy; and D.M.L. and S.F. provided reagents and intellectual input.

Published online at <http://www.nature.com/natureimmunology/>.

Reprints and permissions information is available online at <http://npg.nature.com/reprintsandpermissions/>.

- McNeil, P.L. & Steinhardt, R.A. Plasma membrane disruption: repair, prevention, adaptation. *Annu. Rev. Cell Dev. Biol.* **19**, 697–731 (2003).
- Roy, D. *et al.* A process for controlling intracellular bacterial infections induced by membrane injury. *Science* **304**, 1515–1518 (2004).
- Smith, J. *et al.* Evidence for pore formation in host cell membranes by ESX-1-secreted ESAT-6 and its role in *Mycobacterium marinum* escape from the vacuole. *Infect. Immun.* **76**, 5478–5487 (2008).
- Bi, G.Q., Alderton, J.M. & Steinhardt, R.A. Calcium-regulated exocytosis is required for cell membrane resealing. *J. Cell Biol.* **131**, 1747–1758 (1995).
- Togo, T., Alderton, J.M., Bi, G.Q. & Steinhardt, R.A. The mechanism of facilitated cell membrane resealing. *J. Cell Sci.* **112**, 719–731 (1999).
- Rodriguez, A., Webster, P., Ortego, J. & Andrews, N.W. Lysosomes behave as Ca²⁺-regulated exocytic vesicles in fibroblasts and epithelial cells. *J. Cell Biol.* **137**, 93–104 (1997).
- Martinez, I. *et al.* Synaptotagmin VII regulates Ca²⁺-dependent exocytosis of lysosomes in fibroblasts. *J. Cell Biol.* **148**, 1141–1149 (2000).
- Martens, S. & McMahon, H.T. Mechanisms of membrane fusion: disparate players and common principles. *Nat. Rev. Mol. Cell Biol.* **9**, 543–556 (2008).
- Sudhof, T.C. Synaptotagmins: why so many? *J. Biol. Chem.* **277**, 7629–7632 (2002).
- Craxton, M. & Goedert, M. Alternative splicing of synaptotagmins involving transmembrane exon skipping. *FEBS Lett.* **460**, 417–422 (1999).
- Burgoyne, R.D., O'Callaghan, D.W., Hasdemir, B., Haynes, L.P. & Tepikin, A.V. Neuronal Ca²⁺-sensor proteins: multitalented regulators of neuronal function. *Trends Neurosci.* **27**, 203–209 (2004).
- Bourne, Y., Dannenberg, J., Pollmann, V., Marchot, P. & Pongs, O. Immunocytochemical localization and crystal structure of human frequenin (neuronal calcium sensor 1). *J. Biol. Chem.* **276**, 11949–11955 (2001).
- Haynes, L.P., Thomas, G.M. & Burgoyne, R.D. Interaction of neuronal calcium sensor-1 and ADP-ribosylation factor 1 allows bidirectional control of phosphatidylinositol 4-kinase β and *trans*-Golgi network-plasma membrane traffic. *J. Biol. Chem.* **280**, 6047–6054 (2005).
- Armstrong, J.A. & Hart, P.D. Response of cultured macrophages to *Mycobacterium tuberculosis*, with observations on fusion of lysosomes with phagosomes. *J. Exp. Med.* **134**, 713–740 (1971).
- Schaible, U.E. *et al.* Apoptosis facilitates antigen presentation to T lymphocytes through MHC-I and CD1 in tuberculosis. *Nat. Med.* **9**, 1039–1046 (2003).
- Chen, M. *et al.* Lipid mediators in innate immunity against tuberculosis: opposing roles of PGE₂ and LXA₄ in the induction of macrophage death. *J. Exp. Med.* **205**, 2791–2801 (2008).
- Bafica, A. *et al.* Host control of *Mycobacterium tuberculosis* is regulated by 5-lipoxygenase-dependent lipoxin production. *J. Clin. Invest.* **115**, 1601–1606 (2005).
- Herb, F. *et al.* ALOX5 variants associated with susceptibility to human pulmonary tuberculosis. *Hum. Mol. Genet.* **17**, 1052–1060 (2008).
- Abdallah, A.M. *et al.* Type VII secretion—mycobacteria show the way. *Nat. Rev. Microbiol.* **5**, 883–891 (2007).
- Hsu, T. *et al.* The primary mechanism of attenuation of bacillus Calmette-Guerin is a loss of secreted lytic function required for invasion of lung interstitial tissue. *Proc. Natl. Acad. Sci. USA* **100**, 12420–12425 (2003).
- Chakrabarti, S. *et al.* Impaired membrane resealing and autoimmune myositis in synaptotagmin VII-deficient mice. *J. Cell Biol.* **162**, 543–549 (2003).
- Terasaki, M., Miyake, K. & McNeil, P.L. Large plasma membrane disruptions are rapidly resealed by Ca²⁺-dependent vesicle-vesicle fusion events. *J. Cell Biol.* **139**, 63–74 (1997).
- McNeil, P.L. Incorporation of macromolecules into living cells. *Methods Cell Biol.* **29**, 153–173 (1989).
- Granger, B.L. *et al.* Characterization and cloning of lgp110, a lysosomal membrane glycoprotein from mouse and rat cells. *J. Biol. Chem.* **265**, 12036–12043 (1990).
- Reddy, A., Caler, E.V. & Andrews, N.W. Plasma membrane repair is mediated by Ca²⁺-regulated exocytosis of lysosomes. *Cell* **106**, 157–169 (2001).
- Novikoff, P.M., Tulsiani, D.R., Touster, O., Yam, A. & Novikoff, A.B. Immunocytochemical localization of α -D-mannosidase II in the Golgi apparatus of rat liver. *Proc. Natl. Acad. Sci. USA* **80**, 4364–4368 (1983).
- Hart, D.N., Starling, G.C., Calder, V.L. & Fernando, N.S. B7/BB-1 is a leucocyte differentiation antigen on human dendritic cells induced by activation. *Immunology* **79**, 616–620 (1993).
- Lin, H.Y. *et al.* The 170-kDa glucose-regulated stress protein is an endoplasmic reticulum protein that binds immunoglobulin. *Mol. Biol. Cell* **4**, 1109–1119 (1993).
- Gan, H. *et al.* *Mycobacterium tuberculosis* blocks crosslinking of annexin-1 and apoptotic envelope formation on infected macrophages to maintain virulence. *Nat. Immunol.* **9**, 1189–1197 (2008).
- Chen, M., Gan, H. & Remold, H.G. A mechanism of virulence: virulent *Mycobacterium tuberculosis* strain H37Rv, but not attenuated H37Ra, causes significant mitochondrial inner membrane disruption in macrophages leading to necrosis. *J. Immunol.* **176**, 3707–3716 (2006).
- Klausner, R.D., Donaldson, J.G. & Lippincott-Schwartz, J. Brefeldin A: insights into the control of membrane traffic and organelle structure. *J. Cell Biol.* **116**, 1071–1080 (1992).
- O'Callaghan, D.W. *et al.* Differential use of myristoyl groups on neuronal calcium sensor proteins as a determinant of spatio-temporal aspects of Ca²⁺ signal transduction. *J. Biol. Chem.* **277**, 14227–14237 (2002).
- Togo, T., Alderton, J.M. & Steinhardt, R.A. Long-term potentiation of exocytosis and cell membrane repair in fibroblasts. *Mol. Biol. Cell* **14**, 93–106 (2003).
- Rodriguez, A., Martinez, I., Chung, A., Berlot, C.H. & Andrews, N.W. cAMP regulates Ca²⁺-dependent exocytosis of lysosomes and lysosome-mediated cell invasion by trypanosomes. *J. Biol. Chem.* **274**, 16754–16759 (1999).
- Regan, J.W. EP₂ and EP₄ prostanoid receptor signaling. *Life Sci.* **74**, 143–153 (2003).
- Fujino, H., West, K.A. & Regan, J.W. Phosphorylation of glycogen synthase kinase-3 and stimulation of T-cell factor signaling following activation of EP₂ and EP₄ prostanoid receptors by prostaglandin E₂. *J. Biol. Chem.* **277**, 2614–2619 (2002).
- Simpson, C.S. & Morris, B.J. Induction of c-fos and zif/268 gene expression in rat striatal neurons, following stimulation of D₁-like dopamine receptors, involves protein kinase A and protein kinase C. *Neuroscience* **68**, 97–106 (1995).
- Vlahos, C.J., Matter, W.F., Hui, K.Y. & Brown, R.F. A specific inhibitor of phosphatidylinositol 3-kinase, 2-(4-morpholinyl)-8-phenyl-4H-1-benzopyran-4-one (LY294002). *J. Biol. Chem.* **269**, 5241–5248 (1994).
- Fujino, H., Salvi, S. & Regan, J.W. Differential regulation of phosphorylation of the cAMP response element-binding protein after activation of EP₂ and EP₄ prostanoid receptors by prostaglandin E₂. *Mol. Pharmacol.* **68**, 251–259 (2005).
- Fujino, H., Xu, W. & Regan, J.W. Prostaglandin E₂ induced functional expression of early growth response factor-1 by EP₄, but not EP₂, prostanoid receptors via the phosphatidylinositol 3-kinase and extracellular signal-regulated kinases. *J. Biol. Chem.* **278**, 12151–12156 (2003).
- Hinchey, J. *et al.* Enhanced priming of adaptive immunity by a proapoptotic mutant of *Mycobacterium tuberculosis*. *J. Clin. Invest.* **117**, 2279–2288 (2007).
- Winau, F. *et al.* Apoptotic vesicles crossprime CD8 T cells and protect against tuberculosis. *Immunity* **24**, 105–117 (2006).
- Deretic, V. *et al.* *Mycobacterium tuberculosis* inhibition of phagolysosome biogenesis and autophagy as a host defence mechanism. *Cell. Microbiol.* **8**, 719–727 (2006).
- Vergne, I. *et al.* Mechanism of phagolysosome biogenesis block by viable *Mycobacterium tuberculosis*. *Proc. Natl. Acad. Sci. USA* **102**, 4033–4038 (2005).
- van der Wel, N.N. *et al.* *M. tuberculosis* and *M. leprae* translocate from the phagolysosome to the cytosol in myeloid cells. *Cell* **129**, 1287–1298 (2007).

ONLINE METHODS

Materials. Reagents were as follows: mouse anti-LAMP-1 (1D4B; BD Biosciences); human anti-LAMP-1 (H4A3; Developmental Studies Hybridoma Bank, University of Iowa); anti-mannosidase II (MMS-110R (Covance) and ab12277 (Abcam)); anti-GRP78/BiP (ab21685; Abcam); anti-Syt-7 (105 172; Synaptic Systems); goat anti-mouse immunoglobulin G₁ (A10538; Molecular Probes); mouse immunoglobulin G (641410; BD Biosciences); rabbit anti-annexin-1 (71-3400; Zymed Laboratories); monoclonal murine anti-phosphatidylserine (1H6; Upstate Biotechnology); rabbit immunoglobulin G (Upstate Biotechnology); indocarbocyanine-conjugated donkey anti-rat (Jackson Immuno); anti-CD11b (550282; BD Biosciences); anti-F4/80 (552958; BD Biosciences); monoclonal anti- β -actin (37200; Pierce Biotechnology); PGE₂ (14010; Cayman Chemical); forskolin, brefeldin A, LY294002, KT5720 (Sigma); CD11b MicroBeads (Miltenyi Biotec); and Iscove's modified Dulbecco's medium (IMDM), RPMI-1640 medium, Opti-MEM I, reduced serum medium, oligofectamine, HEPES and dithiothreitol (Invitrogen).

Mice. Six- to ten-week-old C57BL/6 or *Rag1*^{-/-} mice were from Jackson Laboratories; *Alox5*^{-/-} and *Ptges*^{-/-} mice (N₅ backcrossed onto the C57BL/6 background; obtained from B. Koller) were bred locally. All procedures were approved by the Institutional Animal Care and Use Committee of the Dana-Farber Cancer Institute.

Cells and culture. Human studies were approved by the Partners Human Research Committee. Human mononuclear cells from healthy donors were plated at a density of 4×10^5 cells per ml per well in 12-well cluster plates (Corning) for flow cytometry or at 5×10^5 cells/ml/well in 12-well cluster plates for transfection with siRNA. Macrophages were cultured for 7 d in IMDM with 10% (vol/vol) human AB serum (Gemini).

Peritoneal macrophages were collected from wild-type, *Alox5*^{-/-} and *Ptges*^{-/-} mice after being elicited by 3% (vol/vol) thioglycollate, then CD11b⁺ cells were purified with magnetic-activated cell sorting (MACS) columns. For some experiments, mouse spleen macrophages were cultured for 8–10 d in RPMI 1640 medium with 10% (vol/vol) FBS (Gemini), 1% (vol/vol) HEPES, 1% (vol/vol) penicillin-streptomycin and 0.1% (vol/vol) β -mercaptoethanol. Purified cells were over 95% CD11b⁺ and F4/80⁺, as determined by flow cytometry. Macrophages (1×10^5 cells per well) were allowed to adhere for 24 h in a 96-well culture plate.

Bacteria. The virulent Mtb strain Erdman, H37Rv, GFP-labeled H37Rv and the attenuated strain H37Ra (American Type Culture Collection) were prepared as described³⁰ and were grown in Middlebrook 7H9 broth (BD Biosciences) with BBL Middlebrook OADC Enrichment (Becton Dickinson) and 0.05% (vol/vol) Tween 80 (Difco) and the resuspended in 7H9 broth at a density of 5×10^7 CFU/ml. Aggregation was prevented by sonication for 10 s. Bacteria were allowed to settle for 10 min.

In vitro infections. Macrophages were infected with H37Rv or H37Ra at various MOI values as described^{16,46}. At various times, cells were lysed in water for 5 min and mycobacteria were counted by plating of serially dilutions of cell lysates on Middlebrook 7H10 agar plates (REMEL) and culture at 37 °C. Colonies were counted after 21 d.

Aerosol infection of mice. C57BL/6 and *Ptges*^{-/-} mice were infected with H37Rv (Erdman strain) or H37Ra by the aerosol route with a nose-only exposure unit (Intox Products), which delivered approximately 100 CFU per mouse⁴⁷. After 1 week, mice were killed by carbon dioxide inhalation and lungs were removed aseptically and flash-frozen in liquid nitrogen for RNA extraction.

Adoptive transfer model of infection. Peritoneal macrophages were collected from wild-type, *Alox5*^{-/-} and *Ptges*^{-/-} mice after being elicited by 3% (vol/vol) thioglycollate, then CD11b⁺ cells were purified with MACS columns. Suspended macrophages were infected for 30 min *in vitro* at a low MOI (~0.02) of H37Rv. Free bacteria were then removed by six washes with PBS, each followed by centrifugation for 10 min at 200g and 4 °C. Cells were resuspended in PBS at a density of 0.5×10^6 cells per 40 μ l, then were transferred by the intratracheal route⁴⁸ into naive *Rag1*^{-/-} mice. At 2 and 4 weeks after adoptive

transfer, mice were killed and their lungs and spleens were removed and homogenized individually in 0.9% (wt/vol) NaCl–0.02% (vol/vol) Tween 80 with a Mini-BeadBeater-8 (BioSpec Products). Viable bacteria were counted by plating of tenfold serial dilutions of organ homogenates onto 7H11 agar plates (Remel); colonies were counted after 3 weeks of incubation at 37 °C.

Flow cytometry. Cells were stained for 20 min at 37 °C with anti-LAMP-1, anti-GRP78, anti-Syt-7 or anti-mannosidase II in IMDM (20 μ g/ml). After being washed, macrophages were incubated for 20 min at 37 °C with secondary fluorescent rabbit anti-mouse (100 μ g/ml) and were fixed for 20 min at 25 °C with 4% (vol/vol) paraformaldehyde. Cells were dislodged with a rubber policeman, were washed with PBS and were resuspended in PBS with 1% (wt/vol) BSA. A FACSsort flow cytometer (BD Biosciences) was used for flow cytometry.

In vitro assays of necrosis and apoptosis. Necrosis of macrophages *in vitro* was evaluated by flow cytometry according to FDX influx or staining of 7-amino-actinomycin D. Adherent infected and uninfected human macrophages (5×10^5 cells per well) were incubated at 4 °C, then were washed and medium was replaced for 15 min by the same amount of ice-cold IMDM containing FDX (2 mg/ml; relative mass, 75,000). After being washed four times with ice-cold IMDM, cells were fixed overnight with 4% (vol/vol) paraformaldehyde, were scraped off with a rubber policeman, then were washed and were analyzed by flow cytometry. Cells containing more than 30 μ M FDX, as determined by calibration, were gated. Adherent *Ptges*^{-/-} and wild-type spleen macrophages were incubated for 15 min at 37 °C with medium containing 7-amino-actinomycin D (2.5 μ g/ml) and were fixed overnight with 4% (vol/vol) paraformaldehyde. Then macrophages were washed twice with PBS and scraped off the plates, were resuspended in 0.3 ml PBS and were analyzed with a flow cytometer. In some experiments, apoptosis and necrosis were measured by enzyme-linked immunosorbent assay cell (Cell Death Detection ELISA^{PLUS}; 11 920685 001; Roche Applied Science) for quantification of cytoplasmic (apoptosis) and extracellular (necrosis) histone-associated DNA fragments according to the specifications of the manufacturer. The relative amount of necrosis or apoptosis was calculated as a ratio of the absorbance of infected macrophages to that of uninfected control macrophages.

Immunoblot analysis. After incubation with Mtb (MOI, 10), cells were collected and lysed with 1 \times SDS sample buffer (62.5 mM Tris-HCl buffer, pH 6.8, 2% (wt/vol) SDS, 10% (vol/vol) glycerol, 50 mM dithiothreitol, 0.01% (wt/vol) bromophenol blue). Lysates were sonicated for 10 s, centrifuged for 10 min at 10,000g and resolved by 15% SDS-PAGE with β -actin as a loading control. Mouse antibodies were used for the detection of Syt-7 and NCS-1.

Real time PCR. Total RNA from lung tissues or macrophage cultures was isolated with the PureLink Total RNA Purification system (Invitrogen) and was transcribed into cDNA with the Quantitect Reverse Transcription kit (Qiagen) according to the manufacturers' recommendations. The cDNA was denatured for 10 min at 95 °C. Specific DNA fragments were amplified by PCR with a Max3000p Stratagene cyclor with for 40 cycles of 15 s at 95 °C, 60 s at 56 °C and 30 s at 72 °C. The oligonucleotide primers used for mouse β -actin were 5'-AGAGGAAATCGTGGCGTAC-3' (forward) and 5'-CAATAGTGAT GACCTGGC CGT-3' (reverse) and for Syt-7 were 5'-CCGTCAGCCTTAGCGT CAC-3' (forward) and 5'-GCAGGCAACTTGATGGCTTTC-3' (reverse). The amount of amplified Syt-7 DNA fragments was normalized to that of β -actin.

Immunostaining and confocal microscopy. Mouse macrophages were mounted on poly-D lysine-coated coverslips in phenol red-free media and were infected for 24 h with GFP-labeled virulent or avirulent Mtb. Macrophages were then fixed for 30 min with 4% (vol/vol) paraformaldehyde in PBS and were blocked overnight at 4 °C with 10% (vol/vol) horse serum in PBS. Coverslips were incubated for 1 h at 25 °C with anti-LAMP-1 (dilution, 1:10,000). Cells were washed three times with PBS and were stained for 1 h at 25 °C with indocarbocyanine-conjugated donkey anti-rat (dilution, 1:2000). Cells were washed and mounted for imaging. Microscope images were acquired at the Brigham and Women's Confocal Core Facility with a Nikon TE2000-U inverted microscope, Nikon CI Plus confocal system, 60 \times Nikon Plan Apochromat objective, 10-mW Spectra Physics 488-nm argon laser, Melles

Griot Red HeNe 543-nm laser, Chroma 515-nm/30-nm and 543-nm emission filters and a 30- μ m pinhole. Images were acquired in identical exposure conditions and micrographs were compiled and analyzed with Nikon EZ-C1 v3.8 and Adobe Photoshop v10.0.1.

Silencing of the gene encoding human Syt-7 and NCS-1. The human Syt-7-specific siRNA target siRNA sequence (5'-AAGAATGCTAATGTAAAGCAA-3') and the nontargeted siRNA sequence (5'-GAAUUAAGUACAAGUUAGAU-3') were generated by Qiagen. Human NCS-1-specific siRNA (sc-36019) was from Santa Cruz Biotechnology. Cells were cultured in IMDM with 10% (vol/vol) human AB serum and medium was changed 1 d before transfection. All siRNA was used at a final concentration of 50 nM by dilution with Opti-MEM I reduced serum medium. Fresh IMDM containing 30% (vol/vol) human AB serum (Gemini) was added to oligofectamine (1:200 dilution; Invitrogen) to bring the serum concentration to 10%. After transfection for 48 h at 37 °C, cells were infected with Mtb.

Silencing of the gene encoding mouse Syt-7. Primers from the gene encoding mouse Syt-7 (Mouse GeneBank accession number NM-018801) were used to design the siRNA. The sequence of targeted Syt-7 was 5'-CTCCATCATCGT

GAACATCAT-3' (439893; Qiagen). The nontargeted siRNA AllStars (1027280; Qiagen) was used as a negative control. All siRNA was used at a final concentration of 50 nM. Cells were transfected with Hiperfect Transfection Reagent according to the manufacturer's recommendations (Qiagen). For analysis of the effect of siRNA transfection, cells were collected and analyzed with immunoblot or real-time PCR.

Statistics. Data were analyzed with Microsoft Excel Statistical Software (Jandel) with the *t*-test for normally distributed data with equal variances. For some experiments, Prism version 5 for Windows (Graph-Pad Software) was used for one-way ANOVA with Dunnett's post-test and with Bonferroni's post-test.

46. Sada-Ovalle, I., Chiba, A., Gonzales, A., Brenner, M.B. & Behar, S.M. Innate invariant NKT cells recognize *Mycobacterium tuberculosis*-infected macrophages, produce interferon- γ , and kill intracellular bacteria. *PLoS Pathog.* **4**, e1000239 (2008).
47. Woodworth, J.S., Wu, Y. & Behar, S.M. *Mycobacterium tuberculosis*-specific CD8⁺ T cells require perforin to kill target cells and provide protection in vivo. *J. Immunol.* **181**, 8595–8603 (2008).
48. Divangahi, M. *et al.* NOD2-deficient mice have impaired resistance to *Mycobacterium tuberculosis* infection through defective innate and adaptive immunity. *J. Immunol.* **181**, 7157–7165 (2008).